LANDOLT-BÖRNSTEIN

Numerical Data and Functional Relationships in Science and Technology

New Series

Editor in Chief: O. Madelung

Group III: Crystal and Solid State Physics

Volume 22
Semiconductors

Supplements and Extensions to Volume III/17

Editors: O. Madelung · M. Schulz

Subvolume b

Impurities and Defects in Group IV Elements and III-V Compounds

C. A. J. Ammerlaan · W. Bergholz · B. Clerjaud · H. Ennen · H. G. Grimmeiss
B. Hamilton · U. Kaufmann · W. v. Münch · R. Murray · R. C. Newman
A. R. Peaker · G. Pensl · H.-J. Rath · R. Sauer · J. Schneider · M. Schulz
M. S. Skolnick · N. A. Stolwijk · P. Vogl · A. F. W. Willoughby · W. Zulehner

Edited by M. Schulz

Springer-Verlag Berlin Heidelberg New York
London Paris Tokyo Hong Kong

4.2.6 Paramagnetic centers in silicon

4.2.6.1 Introduction

In this section the spectroscopic splitting factors of paramagnetic centers in silicon are given. These **g**-tensors describe the Zeeman splitting of the ground state level in a magnetic field. The energies of the magnetic sub-levels with quantumnumber m_J are found as the eigenvalues of a spin-Hamiltonian operator. Usually the Zeeman interaction $\mathscr{H} = \mu_B \boldsymbol{B} \cdot \mathbf{g} \cdot \boldsymbol{J}$ is the leading term of the spin-Hamiltonian. In this expression μ_B is the Bohr magneton, $\mu_B = 9.274078 \cdot 10^{-24}$ J/T, $\boldsymbol{B}$ is the magnetic field, **g** the **g**-tensor, and $\boldsymbol{J}$ the effective spin. The spin $\boldsymbol{J}$ is compounded from the orbital momentum $\boldsymbol{L}$ and the intrinsic momentum $\boldsymbol{S}$.

Paramagnetic centers in silicon include typical crystal lattice defects, such as radiation damage centers, and impurities, pairs of these entities, and some small aggregates. These centers may destroy none, some, or all of the symmetry elements in the silicon crystal structure. In the first case the full cubic symmetry, pointgroup $\bar{4}3$m as viewed from a substitutional site, is retained. Full destruction of the symmetry operations leads to triclinic symmetry, pointgroup 1. In the intermediate cases some of the symmetry elements are cancelled by the defect while others are left. The seventeen cases compatible with the silicon structure are summarized in Table 1. The pointgroups are grouped into crystallographic systems.

Symmetry invariance imposes constraints on the interaction tensors. The constraints on the principal values and directions of the tensors are given in Table 2, and are illustrated in the Figs. 1b···8b. In the tetragonal and trigonal system two principal g-values are equal resulting in axial symmetry: $g_1 = g_{\parallel}$ and $g_2 = g_3 = g_{\perp}$. In the cubic system all principal g-values are the same and the interaction is isotropic: $g_1 = g_2 = g_3 = g$.

The tensors on their principal axes coordinates can be transformed to the Cartesian (x, y, z)-coordinate system. The transformation formulae are:

$$
\begin{aligned}
g_{xx} &= g_1 g_{1x}^2 + g_2 g_{2x}^2 + g_3 g_{3x}^2, \\
g_{yy} &= g_1 g_{1y}^2 + g_2 g_{2y}^2 + g_3 g_{3y}^2, \\
g_{zz} &= g_1 g_{1z}^2 + g_2 g_{2z}^2 + g_3 g_{3z}^2, \\
g_{xy} &= g_1 g_{1x} g_{1y} + g_2 g_{2x} g_{2y} + g_3 g_{3x} g_{3y}, \\
g_{yz} &= g_1 g_{1y} g_{1z} + g_2 g_{2y} g_{2z} + g_3 g_{3y} g_{3z}, \\
g_{zx} &= g_1 g_{1z} g_{1x} + g_2 g_{2z} g_{2x} + g_3 g_{3z} g_{3x}.
\end{aligned}
$$

The components of the unit vectors of the principal directions are taken from Table 2. Numerical data of principal values and orientations for specific tensors are given in Tables 7···14. The constraints imposed by the higher-symmetry systems on the elements of the Cartesian **g**-tensors are specified in Table 3.

In Table 4, the effective g-values g_{eff} for magnetic field $\boldsymbol{B}$ parallel to [100], [111] and [011] are given for the most general case of the lowest, triclinic, symmetry. For the higher-symmetry systems, the degeneracies of the resonances in these directions are given in Table 5.

There is a one-to-one correspondence between the crystallographic system of the center and the rotation pattern observed in the electron paramagnetic resonance (EPR). For rotation of $\boldsymbol{B}$ in the $(0\bar{1}1)$-plane, which includes the high-symmetry directions [100], [111] and [011], the characteristics of the patterns are given in Table 6. The Figs. 1c···8c illustrate these points. The patterns uniquely define the system and corresponding pointgroup(s).

In the Tables 7···14 the principal values of the **g**-tensors of all, more than 200, observed paramagnetic centers in silicon, arranged according to crystallographic system, are listed. It appears that centers tend to have cubic, trigonal, orthorhombic-I or monoclinic-I symmetry; orthorhombic-II and monoclinic-II symmetry are rare. For the triclinic system, Table 7, unit vectors specify the principal directions g_i, i = 1, 2, 3. Angular information for the monoclinic centers is given by the angle θ, as defined in Table 2 or the Figs. 2b and 3b. Centers within the same crystallographic system are ordered according to increasing trace $(g_1 + g_2 + g_3)/3$ of the **g**-tensor.

4.2.6.2 Symmetry data of defect centers

The following tables present symmetry data of defect centers in silicon:

Table 1. Summary of crystallographic systems and the seventeen pointgroups for centers in the silicon crystal. Pointgroups are labelled by the international symbols, with Schoenflies symbols in parentheses.

System	Pointgroup(s)
Triclinic	1 (C_1), $\bar{1}$ (S_2)
Monoclinic-I	2 (C_2), m (C_v, C_{1h}), 2/m (C_{2h})
Monoclinic-II	2 (C_2)
Orthorhombic-I	2mm (C_{2v})
Orthorhombic-II	222 (D_2)
Tetragonal	$\bar{4}$ (S_4), $\bar{4}$2m (D_{2d})
Trigonal	3 (C_3), $\bar{3}$ (C_{3i}, S_6), 3m (C_{3v}), $\bar{3}$m (D_{3d}), 32 (D_3)
Cubic	23 (T), $\bar{4}$3m (T_d)

Table 2. Constraints on the principal values g_i and directions g_{ix}, g_{iy} and g_{iz}, i=1, 2, 3, of the **g**-tensors for the crystallographic systems.

System	i	g_i	g_{ix}	g_{iy}	g_{iz}	
Triclinic	1	g_1	g_{1x}	g_{1y}	g_{1z}	
	2	g_2	g_{2x}	g_{2y}	g_{2z}	$\mathbf{g}_2 \perp \mathbf{g}_1$
	3	g_3	g_{3x}	g_{3y}	g_{3z}	$\mathbf{g}_3 \perp \mathbf{g}_1$, $\mathbf{g}_3 \perp \mathbf{g}_2$
Monoclinic-I	1	g_1	0	$-1/\sqrt{2}$	$+1/\sqrt{2}$	
	2	g_2	$+\sin\theta$	$-(\cos\theta)/\sqrt{2}$	$-(\cos\theta)/\sqrt{2}$	
	3	g_3	$+\cos\theta$	$+(\sin\theta)/\sqrt{2}$	$+(\sin\theta)/\sqrt{2}$	
Monoclinic-II	1	g_1	+1	0	0	
	2	g_2	0	$+\cos\theta$	$+\sin\theta$	
	3	g_3	0	$-\sin\theta$	$+\cos\theta$	
Orthorhombic-I	1	g_1	+1	0	0	
	2	g_2	0	$+1/\sqrt{2}$	$+1/\sqrt{2}$	
	3	g_3	0	$-1/\sqrt{2}$	$+1/\sqrt{2}$	
Orthorhombic-II	1	g_1	+1	0	0	
	2	g_2	0	+1	0	
	3	g_3	0	0	+1	
Tetragonal	1	$g_\parallel$	+1	0	0	
	2	$g_\perp$	–	–	–	$\mathbf{g}_2 \perp [100]$
	3	$g_\perp$	–	–	–	$\mathbf{g}_3 \perp [100]$, $\mathbf{g}_3 \perp \mathbf{g}_2$
Trigonal	1	$g_\parallel$	$+1/\sqrt{3}$	$+1/\sqrt{3}$	$+1/\sqrt{3}$	
	2	$g_\perp$	–	–	–	$\mathbf{g}_2 \perp [111]$
	3	$g_\perp$	–	–	–	$\mathbf{g}_3 \perp [111]$, $\mathbf{g}_3 \perp \mathbf{g}_2$
Cubic	1	g	g_{1x}	g_{1y}	g_{1z}	
	2	g	–	–	–	$\mathbf{g}_2 \perp \mathbf{g}_1$
	3	g	–	–	–	$\mathbf{g}_3 \perp \mathbf{g}_1$, $\mathbf{g}_3 \perp \mathbf{g}_2$

Table 3. Symmetry-imposed constraints on the elements of the Cartesian **g**-tensor.

System	Relations **g**-tensor elements	
	diagonal	off-diagonal
Triclinic	none	none
Monoclinic-I	$g_{yy}=g_{zz}$	$g_{xy}=g_{zx}$
Monoclinic-II	none	$g_{xy}=g_{zx}=0$
Orthorhombic-I	$g_{yy}=g_{zz}$	$g_{xy}=g_{zx}=0$
Orthorhombic-II	none	$g_{xy}=g_{yz}=g_{zx}=0$
Tetragonal	$g_{yy}=g_{zz}$	$g_{xy}=g_{yz}=g_{zx}=0$
Trigonal	$g_{xx}=g_{yy}=g_{zz}$	$g_{xy}=g_{yz}=g_{zx}$
Cubic	$g_{xx}=g_{yy}=g_{zz}$	$g_{xy}=g_{yz}=g_{zx}=0$

Table 4. Effective g-values g_{eff} for magnetic field $\boldsymbol{B}\|[100]$, labelled S, $\boldsymbol{B}\|[111]$, labelled T, and $\boldsymbol{B}\|[011]$, labelled U, for the general case of triclinic symmetry.

$\boldsymbol{B}\|$	Label	g_{eff}
[100]	S_1	$(g_{xx}^2+g_{xy}^2+g_{zx}^2)^{1/2}$
	S_2	$(g_{yy}^2+g_{yz}^2+g_{xy}^2)^{1/2}$
	S_3	$(g_{zz}^2+g_{zx}^2+g_{yz}^2)^{1/2}$
[111]	T_1	$\{[(g_{xx}+g_{xy}+g_{zx})^2+(g_{yy}+g_{yz}+g_{xy})^2+(g_{zz}+g_{zx}+g_{yz})^2]/3\}^{1/2}$
	T_2	$\{[(g_{xx}-g_{xy}-g_{zx})^2+(g_{yy}+g_{yz}-g_{xy})^2+(g_{zz}-g_{zx}+g_{yz})^2]/3\}^{1/2}$
	T_3	$\{[(g_{xx}-g_{xy}+g_{zx})^2+(g_{yy}-g_{yz}-g_{xy})^2+(g_{zz}+g_{zx}-g_{yz})^2]/3\}^{1/2}$
	T_4	$\{[(g_{xx}+g_{xy}-g_{zx})^2+(g_{yy}-g_{yz}+g_{xy})^2+(g_{zz}-g_{zx}-g_{yz})^2]/3\}^{1/2}$
[011]	U_1	$\{[(g_{yy}+g_{yz})^2+(g_{zz}+g_{yz})^2+(g_{xy}+g_{zx})^2]/2\}^{1/2}$
	U_2	$\{[(g_{yy}-g_{yz})^2+(g_{zz}-g_{yz})^2+(g_{xy}-g_{zx})^2]/2\}^{1/2}$
	U_3	$\{[(g_{zz}+g_{zx})^2+(g_{xx}+g_{zx})^2+(g_{xy}+g_{yz})^2]/2\}^{1/2}$
	U_4	$\{[(g_{zz}-g_{zx})^2+(g_{xx}-g_{zx})^2+(g_{xy}-g_{yz})^2]/2\}^{1/2}$
	U_5	$\{[(g_{xx}+g_{xy})^2+(g_{yy}+g_{xy})^2+(g_{yz}+g_{zx})^2]/2\}^{1/2}$
	U_6	$\{[(g_{xx}-g_{xy})^2+(g_{yy}-g_{xy})^2+(g_{yz}-g_{zx})^2]/2\}^{1/2}$

Table 5. Degeneracies of g_{eff} for magnetic field $\boldsymbol{B}$ parallel to [100], [111], and [011].

System	$\boldsymbol{B}\|[100]$	$\boldsymbol{B}\|[111]$	$\boldsymbol{B}\|[011]$
Triclinic	none	none	none
Monoclinic-I	$S_2=S_3$	$T_3=T_4$	$U_3=U_5$, $U_4=U_6$
Monoclinic-II	none	$T_1=T_2$, $T_3=T_4$	$U_3=U_4$, $U_5=U_6$
Orthorhombic-I	$S_2=S_3$	$T_1=T_2$, $T_3=T_4$	$U_3=U_4=U_5=U_6$
Orthorhombic-II	none	$T_1=T_2=T_3=T_4$	$U_1=U_2$, $U_3=U_4$, $U_5=U_6$
Tetragonal	$S_2=S_3$	$T_1=T_2=T_3=T_4$	$U_1=U_2$, $U_3=U_4=U_5=U_6$
Trigonal	$S_1=S_2=S_3$	$T_2=T_3=T_4$	$U_1=U_3=U_5$, $U_2=U_4=U_6$
Cubic	$S_1=S_2=S_3$	$T_1=T_2=T_3=T_4$	$U_1=U_2=U_3=U_4=U_5=U_6$

Table 6. Number of resonances for the crystallographic systems for various orientations of the magnetic field ***B***.

System	Direction of magnetic field ***B***			
	in {011}-plane	‖⟨100⟩	‖⟨111⟩	‖⟨011⟩
Triclinic	12	3	4	6
Monoclinic-I	7	2	3	4
Monoclinic-II	6	3	2	4
Orthorhombic-I	4	2	2	3
Orthorhombic-II	3	3	1	3
Tetragonal	2	2	1	2
Trigonal	3	1	2	2
Cubic	1	1	1	1

4.2.6.3 Electron paramagnetic resonance (EPR) data

The following tables list data for paramagnetic properties of centers in silicon. Labels as given in the reference literature are used to identify centers of unknown microscopic structure.

Table 7. Principal values and orientations of **g**-tensors of triclinic centers in silicon. For an atomic model, the principal axes of the **g**-tensor and the rotation pattern see Fig. 1.

Label	Spin	i	g_i	g_{ix}	g_{iy}	g_{iz}	Trace	Ref.	Remark
PK2	1/2	1	2.0063	+0.7386	−0.5151	+0.4347	2.0021	86L	[1])
		2	2.0028	+0.5154	+0.8473	+0.1283			
		3	1.9971	−0.4344	+0.1293	+0.8914			
H8	1/2	1	2.0065	+0.749	−0.484	+0.452	2.0022	85D1	
		2	2.0028	+0.495	+0.863	+0.102			
		3	1.9972	−0.439	+0.147	+0.886			
AA3	1/2	1	2.0014	+0.2988	+0.1658	+0.9398	2.0028	83G3	
		2	2.0029	+0.4742	−0.8804	+0.0046			
		3	2.0040	+0.8282	+0.4443	−0.3417			
PK1	1/2	1	2.0082	+0.8819	−0.2093	−0.4225	2.0041	87W	
		2	2.0048	+0.3933	+0.8206	+0.4148			
		3	1.9992	+0.2599	−0.5318	+0.8060			
G10	1/2	1	2.0011	+0.4218	−0.5439	−0.7254	2.0051	76W	
		2	2.0051	+0.1257	−0.7573	+0.6408			
		3	2.0090	+0.8979	+0.3615	+0.2511			
K1	1/2	1	2.0018	+0.2673	+0.8018	−0.5345	2.0061	79W	[2])
		2	2.0092	+0.5488	+0.3293	+0.7683			
		3	2.0074	+0.7921	−0.4987	−0.3520			
AA2	1/2	1	2.0020	+0.2917	+0.7814	+0.5517	2.0063	83G1	[3])
		2	2.0073	+0.7764	−0.5303	+0.3406			
		3	2.0096	+0.5587	+0.3290	−0.7613			
K8	1/2	1	2.0032	+0.3622	+0.7847	+0.5030	2.0072	81W2	[4]) [5])
		2	2.0092	0	+0.5397	−0.8419			
		3	2.0092	−0.9321	+0.3049	+0.1955			
NL23	1/2	1	5.489	+0.1872	+0.8600	−0.4748	3.355	82M	[6])
		2	2.809	+0.9013	−0.3422	−0.2657			
		3	1.768	+0.3921	+0.3782	+0.8386			

[1]) Identical to H8. [2]) Data incomplete. [3]) Data inconsistent. [4]) Similar to K1. [5]) Axial around [18, 39, 25].
[6]) Alternative analysis possible.

Table 8. Principal values and orientations of **g**-tensors of monoclinic-I centers in silicon. For an atomic model, the principal axes of the **g**-tensor, and the rotation pattern see Fig. 2.

Label	Spin	g_1	g_2	g_3	θ	Trace	Ref.	Remark
Au (4)	1/2	1.732	2.243	1.805	10	1.927	83H	
A27	3/2	2.39	1.62	1.96	10	1.99	83C	[1])
G26	1/2	1.9909	2.0084	1.9919	86.4	1.9971	69W	
OS1	1/2	1.9979	1.9929	2.0010	22	1.9973	86W2	
NL3	1/2	2.0000	1.9949	1.9991	23	1.9980	77S	
A18	1/2	2.0023	1.9939	2.0008	20	1.9990	77L	
AA10	1/2	2.0021	1.9943	2.0011	16.6	1.9992	87G3	
G17	1/2	2.0021	2.0001	2.0027	16	2.0016	65W	[2])
G21	1/2	2.0020	2.0008	2.0031	17	2.0020	65W	
G6	1/2	2.0020	2.0004	2.0041	27.6	2.0022	61C	[3])
K7	1/2	2.0135	2.0000	1.9930	22	2.0022	81W1	
A8	1/2	2.0040	2.0035	2.0015	20	2.0030	74L1	[4]) [5])
A10	1/2	2.0042	2.0073	1.9983	25	2.0033	74L1	[6])
H5	1/2	2.0036	2.0065	2.0005	13	2.0035	84D	
G28	1/2	2.0058	2.0019	2.0028	65	2.0035	75W2	
G15	1/2	2.0062	1.9998	2.0052	18.5	2.0037	65W	[7])
A20	1/2	2.0023	2.0084	2.0026	20	2.0044	76L2	
A17	1/2	2.0073	2.0020	2.0050	15	2.0048	77L	
AA4	1/2	2.0060	2.0025	2.0066	31.5	2.0050	85G1	
A6	1/2	2.0028	2.0081	2.0046	20	2.0052	72L1	
NL11	1	2.00945	2.0083	1.9991	33.2	2.0056	78S	
G24	1/2	2.0163	1.9958	2.0058	53.6	2.0060	68E	
P4	1	2.0082	2.0036	2.0066	2.9	2.0061	76L1	[8])
G13	1/2	2.0037	2.0066	2.0086	29	2.0063	65W	
G23	1/2	2.0117	1.9991	2.0081	38.0	2.0063	68E	
A14	1	2.0088	2.0022	2.0087	27.7	2.0066	76L1	[21])
SL2	1/2	2.00807	2.01036	2.00127	57.53	2.0066	72B	[9])
NL12	1/2	2.0103	2.0007	2.0088	57.5	2.0066	78S	
G5	1/2	2.0100	2.0007	2.0096	30	2.0068	65W	
P4	1	2.0090	2.0043	2.0071	3.5	2.0068	63J	[8])
A14	1	2.0090	2.0020	2.0093	33.1	2.0068	82S	[21])
P2	1	2.0088	2.0019	2.0099	32.0	2.0069	76L1	[10])
P3	1	2.0099	2.0010	2.0102	34.4	2.0070	63J	[11])
P2	1	2.0091	2.0023	2.0099	37.2	2.0071	63J	[10])
G8	1/2	2.0112	2.0005	2.0096	32.3	2.0071	59W	[12])
H10	1/2	2.0100	2.0009	2.0103	33.2	2.0071	85D2	
I1	1	2.0094	2.0020	2.0101	32.9	2.0072	79B	[21])
G16	1/2	2.0085	2.0026	2.0107	34.0	2.0073	65W	[13])
S1	1/2	2.0102	2.0011	2.0109	31.5	2.0074	85D2	
K3	1/2	2.0111	2.0022	2.0105	31.5	2.0079	77W	[14])
P1	1/2	2.0117	2.0020	2.0104	32.8	2.0080	62N	[4]) [15]) [16])
K4	1/2	2.0139	2.0000	2.0110	7.0	2.0083	77W	
O1	1/2	2.0130	$\approx$2.001	2.0115	$\approx$35	2.0085	73M	
P1	1/2	2.0125	2.0046	2.0090	17.3	2.0087	63J	[4]) [5]) [16])
G14	1/2	2.0109	2.0019	2.0135	36.7	2.0088	65W	
P1	1/2	2.0127	2.0050	2.0091	15	2.0089	73L	[4]) [16]) [17])
G27	1/2	2.0211	2.0030	2.0035	35	2.0092	69W	
H9	1/2	2.0127	2.0013	2.0144	29.6	2.0095	85D2	

For footnotes see next page. (continued)

Table 8 (continued).

Label	Spin	g_1	g_2	g_3	θ	Trace	Ref.	Remark
G7	1/2	2.0135	2.0012	2.0150	29	2.0099	61C	[18]
G11	1/2	2.0125	2.0076	2.0177	8.2	2.0126	65W	
Ni_i^+	1/2	2.0357	2.0133	2.0333	35.3	2.0274	62L	[19]
L4	1/2	2.037	1.960	2.100	37	2.032	85W2	
A24	1/2	2.0171	1.9775	2.1302	32	2.0416	79L	
NL21	5/2	2.006	2.030	2.100	33.8	2.045	82M	
FeS (I)	1/2	2.126	2.046	2.010	15	2.061	65L	
A28	3/2	2.10	2.05	2.15	15	2.10	83C	[1]
A25	1/2	2.093	2.067	2.153	15	2.104	83C	
A26	1/2	2.131	2.056	2.138	35	2.108	83C	
FeS (III)	1/2	2.042	2.503	1.991	46	2.179	65L	
FeS (IV)	1/2	1.9564	2.6910	1.9390	28.7	2.1955	83S	
FeS (II)	1/2	2.015	2.962	1.938	28.5	2.305	65L	
A27	1/2	4.78	3.24	1.96	10	3.33	83C	
A28	1/2	4.20	4.10	2.15	15	3.48	83C	
NL24	1/2	1.15	9.44	2.06	36.4	4.22	87K	[20]
NL33	1/2	1.472	8.899	2.895	37.3	4.422	86E	
NL21	1/2	4.90	1.961	7.38	33.8	4.75	82M	[1]

[1] Alternative analysis.
[2] Old designation D-center.
[3] Old designation J-center.
[4] Temperature dependent.
[5] Measured at $T = 300$ K.
[6] Similar to G7.
[7] Old designation K-center.
[8] Old designation (V, VI).
[9] Originally designated S2.
[10] Old designation (I, I′).
[11] Old designation (II, III).
[12] Old designation E-center.
[13] Old designation B-center.
[14] K3 related to P1.
[15] Measured at $T = 77$ K.
[16] Old designation N.
[17] Measured at $T = 320$ K.
[18] Old designation C-center.
[19] Measured at $T = 2$ K.
[20] Provisional analysis.
[21] I1 probably identical to A14.

Table 9. Principal values and orientations of **g**-tensors of monoclinic-II centers in silicon. For an atomic model, the principal axes of the **g**-tensor, and the rotation pattern see Fig. 3.

Label	Spin	g_1	g_2	g_3	θ	Trace	Ref.	Remark
PK4	1/2	2.0013	1.9947	2.0030	31	1.9997	86W1	
P6	1/2	2.0040	2.0062	2.0010	17	2.0037	74L2	[1] [2] [3]

[1] Symmetry and constants temperature dependent.
[2] Measured at $T = 200$ K.
[3] Old designation IX.

Table 10. Principal values of **g**-tensors of orthorhombic-I centers in silicon. For an atomic model, the principal axes of the **g**-tensor, and the rotation pattern see Fig. 4.

Label	Spin	g_1	g_2	g_3	Trace	Ref.	Remark
Pt (I)$^-$	1/2	2.0789	1.3867	1.4266	1.6307	62W	
Pt_2	1/2	1.6317	1.5181	2.1869	1.7789	88B	
NL30	1/2	1.9300	1.9471	2.0125	1.9632	86W3	
Pd^-	1/2	2.0544	1.9715	1.9190	1.9816	62W	
NL16	1/2	1.9995	1.9949	1.9995	1.9980	78M	
NL8	1/2	1.99991	1.99323	2.00091	1.99802	78M	[1]
NL2	1/2	1.9978	1.9992	1.9974	1.9981	77S	
NL9	1/2	1.99917	1.99758	1.99847	1.99841	78M	
AA1	1/2	2.0002	1.9954	2.0002	1.9986	83N	
NL10	1/2	1.99959	1.99747	1.99957	1.99888	78M	[1]
NL13	1/2	1.99974	1.99770	1.99949	1.99898	78M	[2]
NL17	1/2	1.99982	1.99799	1.99946	1.99909	78M	[3]
NL14	1/2	1.99966	1.99880	1.99919	1.99922	78M	
U	1/2	1.997	2.002	2.001	2.000	65L	[4]
L6	1/2	2.0029	1.9996	2.0020	2.0015	88W2	
NL7	1/2	2.0032	2.0059	1.9987	2.0026	77S	
GGA1	1/2	2.0039	2.0002	2.0043	2.0028	67W	
I5	1/2	2.0017	2.0086	2.0021	2.0041	76B3	
K2	>1/2	2.0058	2.0004	2.0083	2.0048	76B1	
B1	1/2	2.0029	2.0096	2.0019	2.0048	59B	[5]
B1	1/2	2.0031	2.0093	2.0025	2.0050	61W	[5]
AA7	1	2.0045	2.0008	2.0096	2.0050	87G2	
G12	1/2	2.0068	2.0020	2.0062	2.0050	65W	
K2	>1/2	2.0058	2.0004	2.0094	2.0052	75A	
AA8	1	2.0050	2.0015	2.0094	2.0053	87G2	
AA5	1	2.0056	2.0096	2.0010	2.0054	85G2	
A4	1/2	2.0059	2.0030	2.0094	2.0061	72L1	
AA6	1	2.0067	2.0090	2.0036	2.0064	85G2	
NL1	1/2	2.0047	2.0128	2.0026	2.0067	77S	
P5	1	2.0072	2.0090	2.0051	2.0071	63J	[6]
G2	1/2	2.0038	2.0151	2.0028	2.0072	65W	
G3	1/2	2.0044	2.0143	2.0032	2.0073	65W	
G4	1/2	2.0058	2.0134	2.0027	2.0073	65W	
A16	1/2	2.0071	2.0036	2.0112	2.0073	76L1	
SL1	1	2.0076	2.0102	2.0058	2.0079	71B	[7]
A12	1/2	2.0079	2.0131	2.0030	2.0080	75L	
A15	1	2.0085	2.0045	2.0115	2.0082	76L1	
PK3	1	2.0085	2.0048	2.0118	2.0084	88W1	
I3	1/2	2.0181	2.0209	2.0163	2.0184	76B2	
Ni_i^-	1/2	2.0162	2.0180	2.0533	2.0292	87V	
Au (2)	1/2	2.066	2.260	1.878	2.068	82H	
FeGa (2)	1/2	6.19	0.59	0.69	2.49	88G	
NL28	1/2	5.885	1.236	1.612	2.911	84K	
FeAl (3)	1/2	1.73	2.51	5.36	3.20	88G	
FeGa (3)	1/2	2.02	3.37	4.65	3.35	88G	
(FeIn)°	1/2	2.07	3.78	4.40	3.42	62L	
NL32	1/2	7.902	1.811	4.184	4.632	86E	

[1]) g-Values time dependent [79M], superposition of several spectra.
[2]) Later annealing stage of NL10.
[3]) Later annealing stage of NL10 and NL13 [87G1].
[4]) Provisional analysis.
[5]) Old designation A-center.
[6]) Old designation (VII, VIII).
[7]) Originally designated S1.

Table 11. Principal values of **g**-tensors of orthorhombic-II centers in silicon. For an atomic model, the principal axes of the **g**-tensor, and the rotation pattern see Fig. 5.

Label	Spin	g_1	g_2	g_3	Trace	Ref.	Remark
NL25	5/2	2.51	1.47	0.57	1.52	82M	[1]
P6	1/2	2.0009	2.0032	2.0054	2.0032	63J	[2] [3] [4]
P6	1/2	2.0015	2.0038	2.0056	2.0036	74L2	[2] [3] [5]
NL24	5/2	3.66	3.93	2.12	3.24	82M	[1]

[1] Provisional analysis, actual symmetry lower.
[2] Old designation IX.
[3] Temperature dependent.
[4] Measured at $T=300$ K.
[5] Measured at $T=315$ K.

Table 12. Principal values of **g**-tensors of tetragonal centers in silicon. For an atomic model, the principal axes of the **g**-tensor, and the rotation pattern see Fig. 6.

Label	Spin	$g_{\parallel}$	$g_{\perp}$	Trace	Ref.	Remark
In	1/2	0.98	1.57	1.37	60F	[1]
Ga	1/2	1.14	2.04	1.74	60F	[1]
Al	1/2	1.18	2.16	1.83	60F	[1]
LiX	1/2	1.9993	1.9987	1.9989	70W	
Li	1/2	1.9997	1.9987	1.9990	70W	
O2	1/2	2.0005	2.0020	2.0015	75M	
G1	1/2	2.0087	1.9989	2.0022	63W	
SL3	1/2	2.0027	2.0023	2.0024	73B1	
G25	1/2	2.0089	2.0006	2.0034	75W1	
A5	1	2.0066	2.0064	2.0065	72L1	
L1	1/2	2.0039	1.9991	2.0007	85H	
B3	1/2	2.0159	2.0051	2.0087	71D	
SL4	1/2	2.0165	2.0053	2.0090	74B	[2]
B	1/2	1.21	2.43	2.02	60F	[1]

[1] Large external uniaxial compressive stress along [100].
[2] Identical to B3, notation SL4 discontinued [78B].

Table 13. Principal values of **g**-tensors of trigonal centers in silicon. For an atomic model, the principal axes of the **g**-tensor, and the rotation pattern see Fig. 7.

Label	Spin	$g_{\parallel}$	$g_{\perp}$	Trace	Ref.	Remark
$(CrAl)^{\circ}$	5/2	1.994	1.994	1.994	62L	
NL4	1/2	1.9957	1.9988	1.9978	77S	
$(CrGa)^{\circ}$	5/2	1.995	1.999	1.998	62L	
$(MnZn)^{\circ}$	5/2	2.001	1.996	1.998	62L	
$(Mg^{+})^{*}$	1/2	1.9974	1.9986	1.9982	73B2	
$(LiO)^{\circ}$	1/2	1.9978	1.9992	1.9987	59F	
G22	1/2	2.0014	1.9973	1.9987	65W	
AA9	1/2	2.0011	1.9983	1.9992	87G3	
L7	1/2	2.0008	1.9994	1.9999	88S	[10]
$(CrB)^{\circ}$	5/2	2.0	2.0	2.0	62L	
G19	1/2	2.0006	2.0009	2.0008	65W	

(continued)

Table 13 (continued).

Label	Spin	$g_{\parallel}$	$g_{\perp}$	Trace	Ref.	Remark
NL31	1/2	2.00250	2.00034	2.00106	88O	
G20	1/2	2.0014	2.0025	2.0021	65W	
Se_2^+	1/2	2.0020	2.0039	2.0033	84W	
(CrAu)°	3/2	2.015	1.999	2.004	62L	
(CrCu)°	3/2	2.003	2.0045	2.004	87S	
$(MnB)^+$	5/2	2.0041	2.0041	2.0041	82K1	
$(MnAl)^+$	5/2	2.003	2.006	2.005	62L	
$(MnAu)^+$	3/2	2.003	2.006	2.005	62L	
B4	1/2	2.0007	2.0073	2.0051	71D	
A19	1/2	2.0076	2.0039	2.0051	76L2	
G29	1	2.0107	2.0025	2.0052	75W3	
A2	1/2	2.0074	2.0044	2.0054	72L1	
K9	1/2	2.0008	2.0086	2.0060	83W	[1])
SL6	1/2	2.0018	2.0085	2.0063	81B	
H11	1/2	2.0022	2.0084	2.0063	86D1	
SL5	1/2	2.0026	2.0089	2.0068	80B	
GGA3	1/2	2.0022	2.0091	2.0068	69H	
B2	1/2	2.0008	2.0100	2.0069	69D	[2])
A1	1/2	2.0018	2.0096	2.0070	72L1	[3])
G8	1/2	2.0081	2.0064	2.0070	72L2	[4])
S1	1/2	2.0010	2.0103	2.0072	67L1	[5])
P7	1/2	2.0028	2.0104	2.0079	65H	[6])
A3	1/2	2.0029	2.0104	2.0079	72L1	[6])
$(MnAu)^-$	5/2	1.991	2.016	2.008	62L	
A7	1/2	1.9914	2.0165	2.0081	72L1	
K5	1/2	2.0020	2.0124	2.0089	77W	
G7	1/2	2.0116	2.0079	2.0091	72L2	[7])
A9	1/2	2.0049	2.0112	2.0091	74L1	
G9	1	2.0136	2.0085	2.0102	65W	
$(MnCu)^+$	3/2	2.0065	2.016	2.013	86D2	
(MnPt)°	3/2	2.027	2.017	2.020	62L	
$(MnCu)^-$	3/2	2.0130	2.025	2.021	86D2	
(FeB)°	3/2	2.068	2.0	2.023	62L	
A22	3/2	2.1001	2.0132	2.0422	79L	[8])
(FeB)°	3/2	2.0676	2.0452	2.0527	83G2	
NL22	4	2.075	2.068	2.070	82M	
NL20	5/2	2.059	2.078	2.072	82M	[8])
Pt (II)	1/2	2.021	2.126	2.091	62W	
Au (5)	1/2	1.8517	2.2143	2.0934	86H	
NL19	3/2	2.1163	2.0935	2.1011	82M	
A23	1/2	2.0993	2.1165	2.1108	81K	
A23	1/2	2.1001	2.1178	2.1119	79L	[9])
Au (1)	1/2	2.1005	2.1183	2.1124	80H	
NL27	1/2	6.389	1.138	2.888	84K	
(CrAu)°	1/2	2.0145	3.9817	3.3260	60W2	[8])
(FeGa)°	1/2	5.089	2.530	3.383	60L	
A22	1/2	2.1001	4.0264	3.3843	79L	[8])
NL20	1/2	2.059	6.235	4.843	82M	[8])

[1]) Similar to B4.
[2]) Identical to S1.
[3]) Similar to motionally averaged G8.
[4]) Motionally averaged state at $T = 300$ K.
[5]) See analysis spectrum S1, monoclinic-I [85D2].
[6]) A3 identical to P7.
[7]) Motionally averaged state at $T = 90$ K.
[8]) Alternative analysis.
[9]) Identical to Au(1).
[10]) Motionally averaged state at $T > 15$K.

Table 14. Principal values of **g**-tensors of cubic centers in silicon. For an atomic model, the principal axes of the **g**-tensor, and the rotation pattern see Fig. 8.

Label	Spin	g	Trace	Ref.	Remark
Ga	3/2	0.994	0.994	81N	[1])
Al	3/2	0.998	0.998	81N	[1])
In	3/2	1.031	1.031	82K2	[1])
B	3/2	1.071	1.071	78N	[1])
(Mn_i^+)**	3	1.34	1.34	62L	[2])
(Mn_i°)*	3/2	1.46	1.46	62L	[2])
(Mn_i^+)*	2	1.68	1.68	62L	[2])
(Cr_i°)*	2	1.72	1.72	62L	[2])
V_i^{2+}	3/2	1.9892	1.9892	60W1	
Cr_s°	1	1.9962	1.9962	62L	
Cr_i^+	5/2	1.9978	1.9978	60W1	
NL29	3/2	1.99806	1.99806	85W1	
Mg^+	1/2	1.9981	1.9981	73B2	
NL6	1/2	1.9982	1.9982	77S	
As	1/2	1.99837	1.99837	59F	
P	1/2	1.99850	1.99850	59F	
RCA2	1/2	1.9985	1.9985	66G	
Sb	1/2	1.99858	1.99858	59F	
NL5	1/2	1.9986	1.9986	77S	
CE	1/2	1.99875	1.99875	59F	[3])
A21	1/2	1.9992	1.9992	79L	
NL15	1/2	1.99926	1.99926	78M	
NL18	1/2	1.99944	1.99944	78M	
RCA1	1/2	1.9996	1.9996	66G	
Bi	1/2	2.0003	2.0003	59F	
S_2^+	1/2	2.0008	2.0008	65L	[4])
G18	1/2	2.0019	2.0019	65W	
NL26	1/2	2.0022	2.0022	84S	
Htc	1/2	2.0023	2.0023	59F	
Te^+	1/2	2.0023	2.0023	81G	
A13	1/2	2.0023	2.0023	74L3	
GGA2	1/2	2.0029	2.0029	67W	
A11	1/2	2.0034	2.0034	74L1	
Au (3)	1/2	2.0045	2.0045	82H	
RCA3	1/2	2.0046	2.0046	70G	
S^+	1/2	2.0054	2.0054	65L	
a	1/2	2.0055	2.0055	69B	[3])
Se^+	1/2	2.0057	2.0057	81G	
Mn_s^{2-}	5/2	2.0058	2.0058	60W3	
N (1)	1/2	2.0061	2.0061	72M	
$(Mn_i)_4^\circ$	2	2.0063	2.0063	59L	
SL5	1/2	2.0065	2.0065	83M	[5])
Mn_i^{2+}	5/2	2.0066	2.0066	60W1	
S2	1/2	2.0069	2.0069	67L2	
RCA4	1/2	2.0090	2.0090	70G	
Mn_i^-	1	2.0104	2.0104	60W1	
Mn_s^+	1	2.0259	2.0259	60W3	
Ni_i^+	1/2	2.026	2.026	62L	[6])

[1]) Sign g-value negative.
[2]) Excited state.
[3]) Isotropic.
[4]) Symmetry cubic within limits of resolution.
[5]) Motionally averaged state at room temperature.
[6]) Motionally narrowed spectrum at $T = 10 \cdots 20$ K.

(continued)

Table 14 (continued).

Label	Spin	g	Trace	Ref.	Remark
N (2)	1/2	2.041	2.041	72M	
Zn^-	1/2	2.050	2.050	72G	
Fe_i°	1	2.0699	2.0699	58L	
Cr_i°	1	2.97	2.97	62L	
Mn_i^+	1	3.01	3.01	62L	
Mn_i°	1/2	3.362	3.362	62L	
Fe_i^+	1/2	3.524	3.524	60L	

Figures for 4.2.6

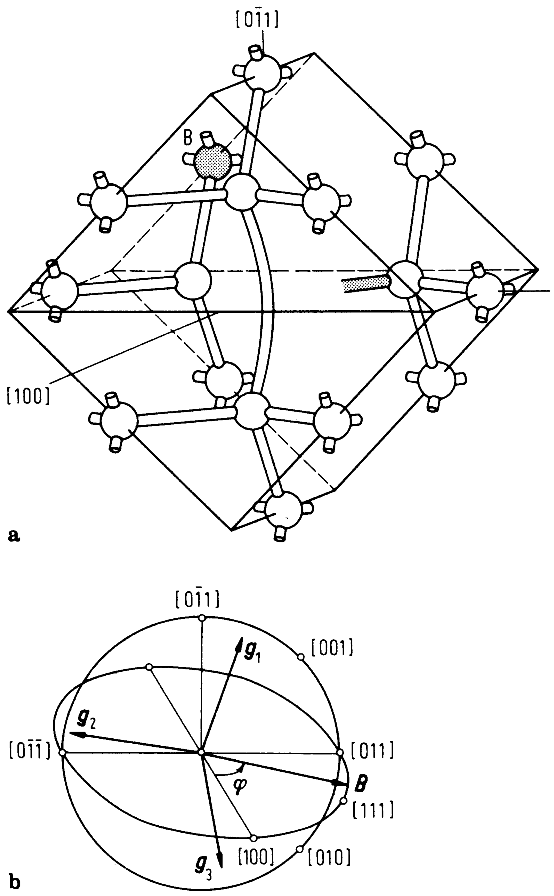

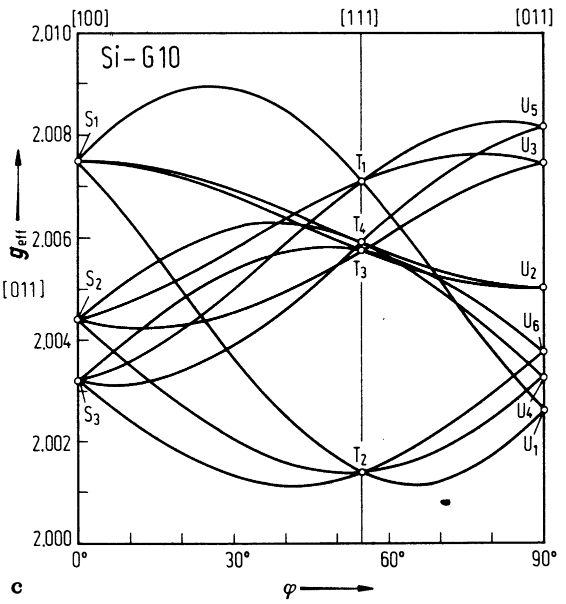

Fig. 1a···c. Triclinic system. (a) Atomic model boron-vacancy complex in silicon, pointgroup 1. (b) Principal axes of the triclinic **g**-tensor. (c) Rotation pattern spectrum Si-G10, $\boldsymbol{B}$ in the (0$\bar{1}$1)-plane.

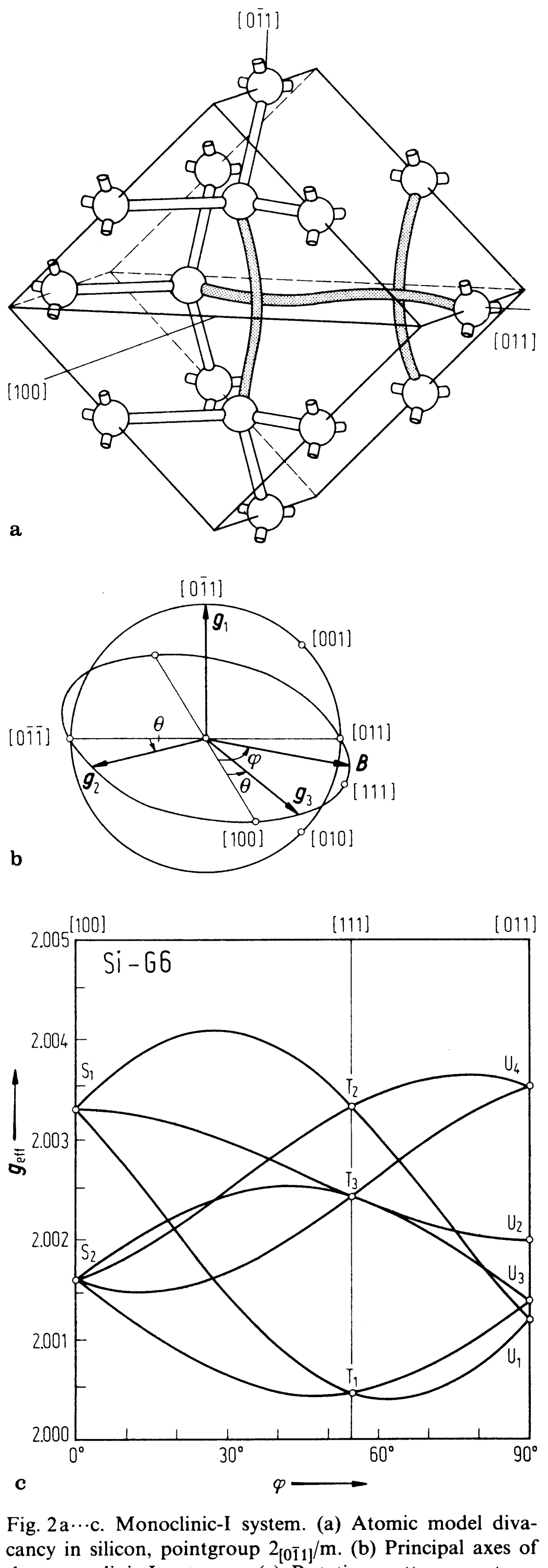

Fig. 2a···c. Monoclinic-I system. (a) Atomic model divacancy in silicon, pointgroup $2_{[0\bar{1}1]}/m$. (b) Principal axes of the monoclinic-I **g**-tensor. (c) Rotation pattern spectrum Si-G6, ***B*** in the (0$\bar{1}$1)-plane.

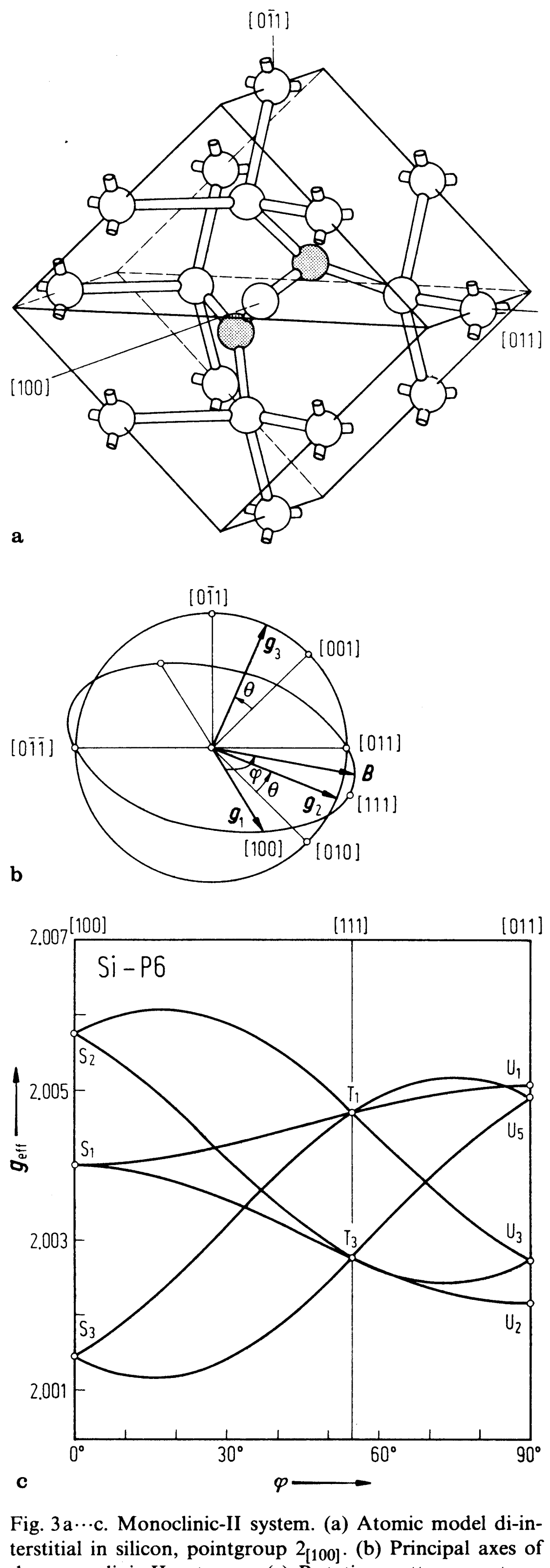

Fig. 3a···c. Monoclinic-II system. (a) Atomic model di-interstitial in silicon, pointgroup $2_{[100]}$. (b) Principal axes of the monoclinic-II **g**-tensor. (c) Rotation pattern spectrum Si-P6 (T = 200 K), ***B*** in the (0$\bar{1}$1)-plane.

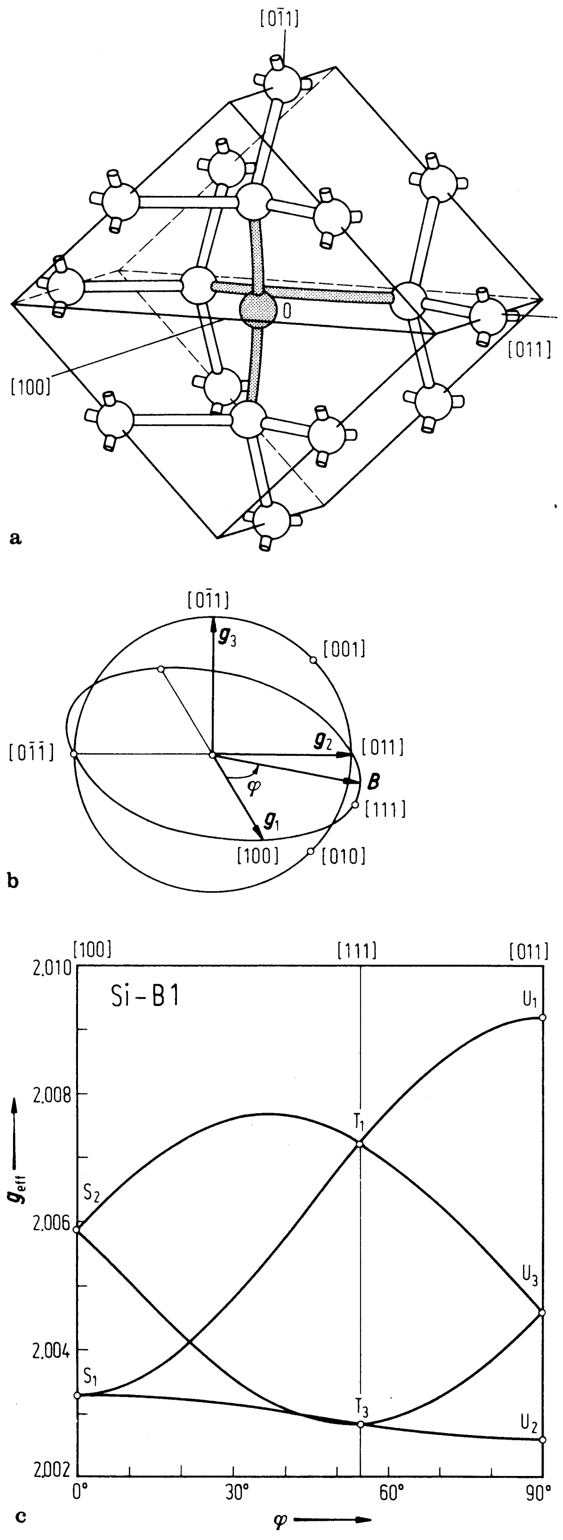

Fig. 4a···c. Orthorhombic-I system. (a) Atomic model oxygen-vacancy complex in silicon, pointgroup $2_{[100]}mm$. (b) Principal axes of the orthorhombic-I **g**-tensor. (c) Rotation pattern spectrum Si-B1, ***B*** in the $(0\bar{1}1)$-plane.

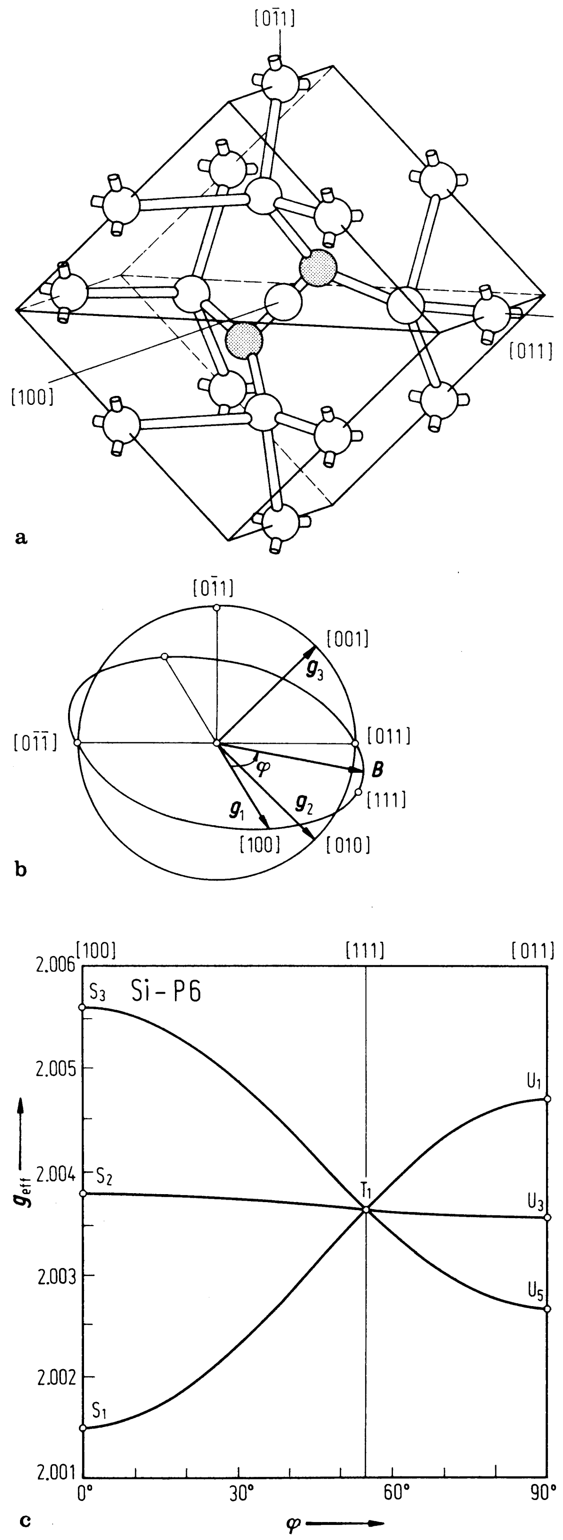

Fig. 5a···c. Orthorhombic-II system. (a) Atomic model di-interstitial in silicon, pointgroup 222. (b) Principal axes of the orthorhombic-II **g**-tensor. (c) Rotation pattern spectrum Si-P6 (T = 315 K), ***B*** in the $(0\bar{1}1)$-plane.

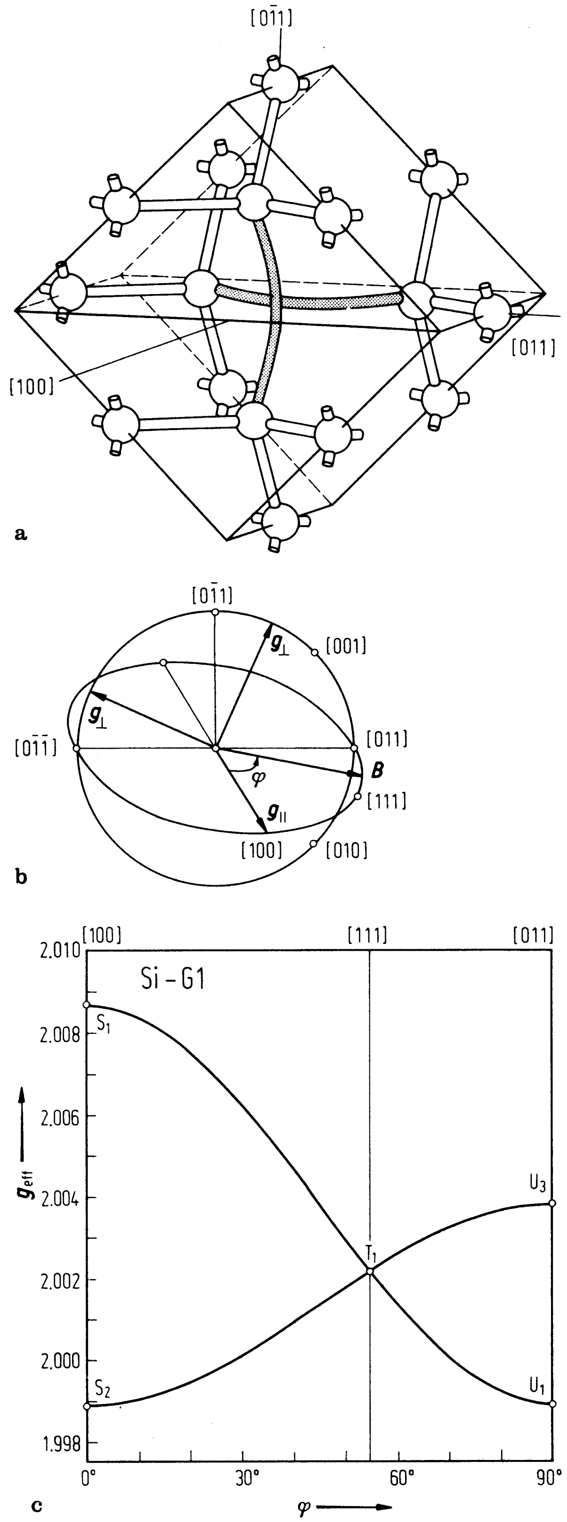

Fig. 6a···c. Tetragonal system. (a) Atomic model positive vacancy in silicon, pointgroup $\bar{4}_{[100]}2m$. (b) Principal axes of the tetragonal **g**-tensor. (c) Rotation pattern spectrum Si-G1, $\boldsymbol{B}$ in the (0$\bar{1}$1)-plane.

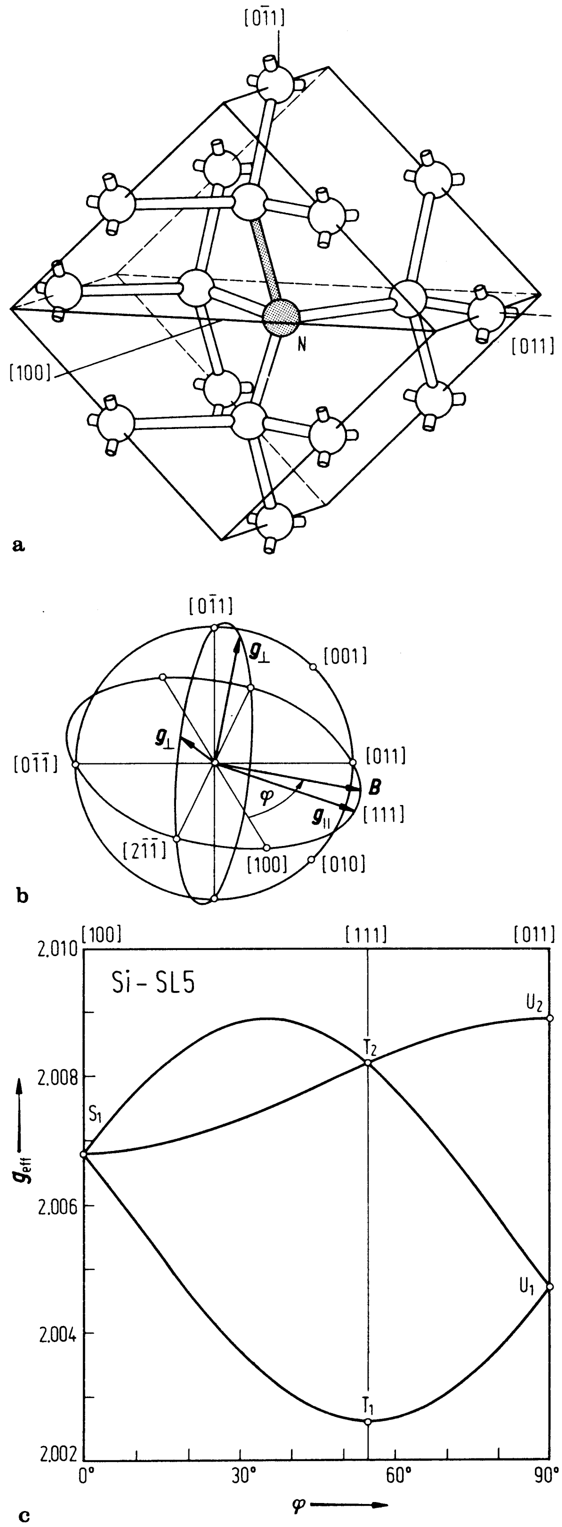

Fig. 7a···c. Trigonal system. (a) Atomic model nitrogen in silicon, pointgroup 3m. (b) Principal axes of the trigonal **g**-tensor. (c) Rotation pattern spectrum Si-SL5, $\boldsymbol{B}$ in the (0$\bar{1}$1)-plane.

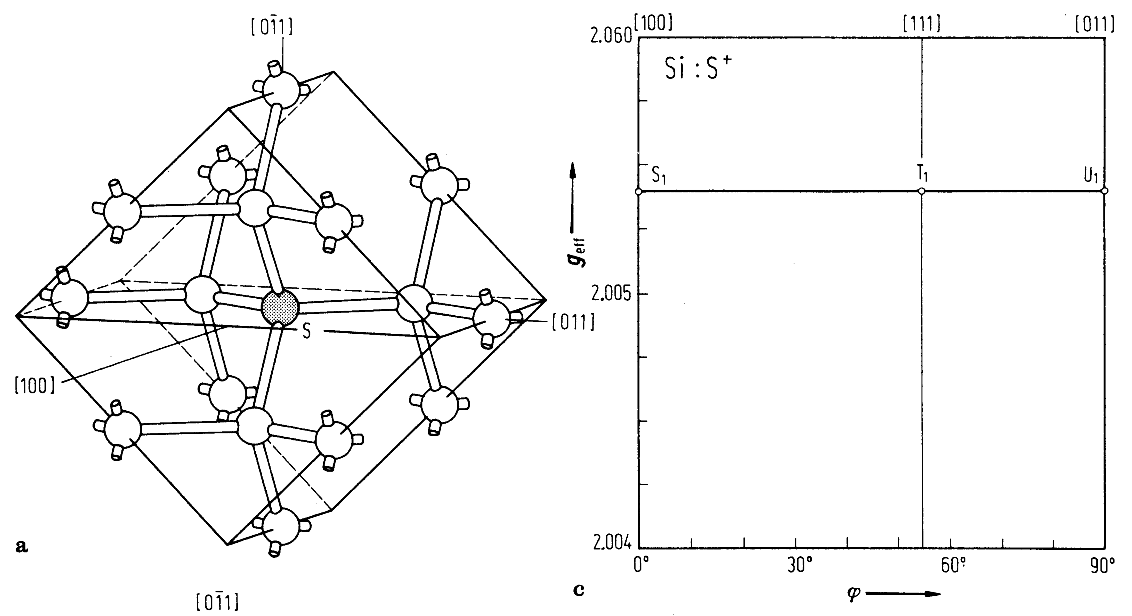

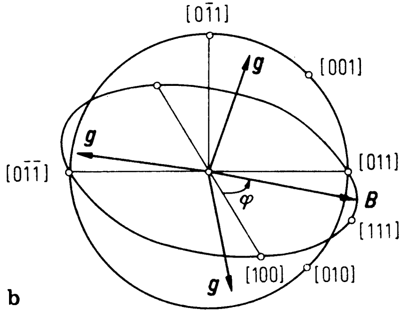

Fig. 8a···c. Cubic system. (a) Atomic model of sulfur in silicon, pointgroup $\bar{4}$3m. (b) Principal axes of the cubic **g**-tensor. (c) Rotation pattern spectrum Si:S$^+$, ***B*** in the (0$\bar{1}$1)-plane.

References for 4.2.6

58L Ludwig, G.W., Woodbury, H.H., Carlson, R.O.: Phys. Rev. Lett **1** (1958) 295.
59B Bemski, G.: J. Appl. Phys. **30** (1959) 1195.
59F Feher, G.: Phys. Rev. **114** (1959) 1219.
59L Ludwig, G.W., Woodbury, H.H., Carlson, R.O.: J. Phys. Chem. Solids **8** (1959) 490.
59W Watkins, G.D., Corbett, J.W., Walker, R.M.: J. Appl. Phys. **30** (1959) 1198.
60F Feher, G., Hensel, J.C., Gere, E.A.: Phys. Rev. Lett. **5** (1960) 309.
60L Ludwig, G.W., Woodbury, H.H.: Phys. Rev. **117** (1960) 1286.
60W1 Woodbury, H.H., Ludwig, G.W.: Phys. Rev. **117** (1960) 102.
60W2 Woodbury, H.H., Ludwig, G.W.: Phys. Rev. **117** (1960) 1287.
60W3 Woodbury, H.H., Ludwig, G.W.: Phys. Rev. Lett. **5** (1960) 96.
61C Corbett, J.W., Watkins, G.D.: Phys. Rev. Lett. **7** (1961) 314.
61W Watkins, G.D., Corbett, J.W.: Phys. Rev. **121** (1961) 1001.
62L Ludwig, G.W., Woodbury, H.H.: Solid State Phys. **13** (1962) 223.
62N Nisenoff, M., Fan, H.Y.: Phys. Rev. **128** (1962) 1605.
62W Woodbury, H.H., Ludwig, G.W.: Phys. Rev. **126** (1962) 466.
63J Jung, W., Newell, G.S.: Phys. Rev. **132** (1963) 648.
63W Watkins, G.D.: J. Phys. Soc. Jpn. **18**, Suppl. II (1963) 22.
65H Hale, E.B.: Semiconductor Research Semiannual Report, Purdue University, USA **1965**, p. 20.
65L Ludwig, G.W.: Phys. Rev. **137** (1965) A1520.
65W Watkins, G.D.: Radiation Damage in Semiconductors, Paris: Dunod **1965**, p. 97.
66G Goldstein, B.: Phys. Rev. Lett. **17** (1966) 428.

67L1 Lütgemeier, H., Schnitzke, K.: Phys. Lett. **25A** (1967) 232.
67L2 Lütgemeier, H., Schnitzke, K.: Phys. Lett. **25A** (1967) 726.
67W Wikner, E.G., Horiye, H.: Bull. Am. Phys. Soc. Ser. II, **12** (1967) 346.
68E Elkin, E.L., Watkins, G.D.: Phys. Rev. **174** (1968) 881.
69B Brodsky, M.H., Title, R.S.: Phys. Rev. Lett. **23** (1969) 581.
69D Daly, D.F., Pickar, K.A.: Appl. Phys. Lett. **15** (1969) 267.
69H Horiye, H., Wikner, E.G.: J. Appl. Phys. **40** (1969) 3879.
69W Watkins, G.D.: private communication **1969**.
70G Goldstein, B.: Phys. Rev. **B2** (1970) 4110.
70W Watkins, G.D., Ham, F.S.: Phys. Rev. **B1** (1970) 4071.
71B Brower, K.L.: Radiat. Eff. **8** (1971) 213.
71D Daly, D.F.: J. Appl. Phys. **42** (1971) 864.
72B Brower, K.L., Beezhold, W.: J. Appl. Phys. **43** (1972) 3499.
72G Ginodman, V.B., Gladkov, P.S., Zhurkin, B.G., Kornilov, B.V.: Sov. Phys. Semicond. **5** (1972) 1930.
72L1 Lee, Y.H., Kim, Y.M., Corbett, J.W.: Radiat. Eff. **15** (1972) 77.
72L2 Lee, Y.H.: Thesis, State University of New York at Albany, USA **1972**.
72M Matsumori, T., Takeda, K., Kobayashi, T., Maekawa, H., Izumi, T.: Tokai Daigaku Kiyo Kogakubu **1** (1972) 1.
73B1 Beezhold, W., Brower, K.L.: IEEE Trans. Nucl. Sci. NS-**20** (1973) 209.
73B2 Baxter, J.E., Ascarelli, G.: Phys. Rev. **B7** (1973) 2630.
73L Lee, Y.H., Corbett, J.W.: Phys. Rev. **B8** (1973) 2810.
73M Murakami, K., Masuda, K., Gamo, K., Namba, S.: Jpn. J. Appl. Phys. **12** (1973) 1307.
74B Brower, K.L.: Phys. Rev. **B9** (1974) 2607.
74L1 Lee, Y.H., Brosious, P.R., Corbett, J.W.: Radiat. Eff. **22** (1974) 169.
74L2 Lee, Y.H., Corbett, J.W.: Solid State Commun. **15** (1974) 1781.
74L3 Lee, Y.H., Brosious, P.R., Corbett, J.W.: Phys. Lett. **49A** (1974) 425.
75A Alexander, H., Kenn, M., Nordhofen, B., Weber, E., Sander, W.: Inst. Phys. Conf. Ser. **23** (1975) 433.
75L Lee, Y.H., Brosious, P.R., Cheng, L.J., Corbett, J.W.: Ion Implantation in Semiconductors, New York: Plenum Press **1975**, p. 519.
75M Murakami, K., Masuda, K., Gamo, K., Namba, S.: Ion Implantation in Semiconductors, New York: Plenum Press **1975**, p. 533.
75W1 Watkins, G.D.: Inst. Phys. Conf. Ser. **23** (1975) 1.
75W2 Watkins, G.D.: Phys. Rev. **B12** (1975) 5824.
75W3 Watkins, G.D.: Phys. Rev. **B12** (1975) 4383.
76B1 Bartelsen, L.: Thesis, University of Köln, West-Germany **1976**.
76B2 Brosious, P.R.: Appl. Phys. Lett. **29** (1976) 265.
76B3 Brosious, P.R.: Proc. 5th Ion Implantation Conference, Boulder, USA **1976**, p. 417.
76L1 Lee, Y.H., Corbett, J.W.: Phys. Rev. **B13** (1976) 2653.
76L2 Lee, Y.H.: private communication **1976**.
76W Watkins, G.D.: Phys. Rev. **B13** (1976) 2511.
77L Lee, Y.H., Corelli, J.C., Corbett, J.W.: Phys. Lett. **60A** (1977) 55.
77S Sieverts, E.G., Ammerlaan, C.A.J.: Inst. Phys. Conf. Ser. **31** (1977) 213.
77W Weber, E., Alexander, H.: Inst. Phys. Conf. Ser. **31** (1977) 266.
78B Brower, K.L.: Phys. Rev. **B17** (1978) 4130.
78M Muller, S.H., Sprenger, M., Sieverts, E.G., Ammerlaan, C.A.J.: Solid State Commun. **25** (1978) 987.
78N Neubrand, H.: Phys. Status Solidi (b) **86** (1978) 269.
78S Sieverts, E.G., Muller, S.H., Ammerlaan, C.A.J.: Solid State Commun. **28** (1978) 221.
79B Brosious, P.R.: Inst. Phys. Conf. Ser. **46** (1979) 248.
79L Lee, Y.H., Kleinhenz, R.L., Corbett, J.W.: Inst. Phys. Conf. Ser. **46** (1979) 521.
79M Muller, S.H., Sieverts, E.G., Ammerlaan, C.A.J.: Inst. Phys. Conf. Ser. **46** (1979) 297.
79W Weber, E., Alexander, H.: J. Phys. Colloq. C6, **40** (1979) 101.
80B Brower, K.L.: Phys. Rev. Lett. **44** (1980) 1627.
80H Höhne, M.: Phys. Status Solidi (b) **99** (1980) 651.
81B Brower, K.L.: Inst. Phys. Conf. Ser. **59** (1981) 491.
81G Grimmeiss, H.G., Janzén, E., Ennen, H., Schirmer, O.F., Schneider, J., Wörner, R., Holm, C., Sirtl, E., Wagner, P.: Phys. Rev. **B24** (1981) 4571.

81K Kleinhenz, R.L., Lee, Y.H., Corbett, J.W., Sieverts, E.G., Muller, S.H., Ammerlaan, C.A.J.: Phys. Status Solidi (b) **108** (1981) 363.
81N Neubrand, H.: private communication **1981**.
81W1 Weber, E., Alexander, H.: Solid State Commun. **37** (1981) 371.
81W2 Weber, E.: Cryst. Res. & Technol. **16** (1981) 209.
82H Höhne, M.: Phys. Status Solidi (b) **109** (1982) 525.
82K1 Kreissl, J., Gehlhoff, W.: Phys. Status Solidi (b) **112** (1982) 695.
82K2 van Kemp, R.: private communication **1982**.
82M Muller, S.H., Tuynman, G.M., Sieverts, E.G., Ammerlaan, C.A.J.: Phys. Rev. **B25** (1982) 25.
82S Sieverts, E.G., Corbett, J.W.: Solid State Commun. **43** (1982) 41.
83C Corbett, J.W.: private communication **1983**.
83G1 Gorelkinskii, Yu.V., Nevinnyi, N.N.: Phys. Lett. **99A** (1983) 117.
83G2 Gehlhoff, W., Segsa, K.H.: Phys. Status Solidi (b) **115** (1983) 443.
83G3 Gorelkinskii, Yu. V., Nevinnyi, N.N.: Ion Implantation in Semiconductors and Other Materials, Vilnius, USSR **1983**, p. 59.
83H Höhne, M.: Phys. Status Solidi (b) **119** (1983) K117.
83M Murakami, K., Masuda, K., Aoyagi, Y., Namba, S.: Physica **116B** (1983) 564.
83N Nevinnyi, N.N., Gorelkinskii, Yu. V.: Ion Implantation in Semiconductors and Other Materials, Vilnius, USSR **1983**, p. 61.
83S Schirmer, O.F.: Physica **116B** (1983) 306.
83W Weber, E.R.: Appl. Phys. A **30** (1983) 1.
84D Dvurechenskii, A.V., Kashnikov, B.P., Suprunchik, V.V.: Phys. Status Solidi (a) **86** (1984) 313.
84K van Kooten, J.J., Weller, G.A., Ammerlaan, C.A.J.: Phys. Rev. **B30** (1984) 4564.
84S Sprenger, M., Sieverts, E.G., Muller, S.H., Ammerlaan, C.A.J.: Solid State Commun. **51** (1984) 951.
84W Wörner, R., Schirmer, O.F.: Solid State Commun. **51** (1984) 665.
85D1 Dvurechenskii, A.V., Suprunchik, V.V.: Phys. Status Solidi (a) **92** (1985) K53.
85D2 Dvurechenskii, A.V., Karanovich, A.A.: Sov. Phys. Semicond. **19** (1985) 1198.
85G1 Gorelkinskii, Yu.V., Nevinnyi, N.N., Kim, A.A.: Phys. Status Solidi (b) **130** (1985) K51.
85G2 Gorelkinskii, Yu.V., Nevinnyi, N.N., Ajazbaev, S.S.: Phys. Lett. **110A** (1985) 157.
85H Harris, R.D., Watkins, G.D.: J. Electron. Mater. **14a** (1985) 799.
85W1 van Wezep, D.A., Ammerlaan, C.A.J.: J. Electron. Mater. **14a** (1985) 863.
85W2 Weber, J., Watkins, G.D.: J. Electron. Mater. **14a** (1985) 661.
86D1 Dvurechenskii, A.V., Suprunchik, V.V.: Institute Semiconductor Physics, Novosibirsk, USSR **1986**.
86D2 Dietrich, H., Vollmer, H., Labusch, R.: Solid State Commun. **58** (1986) 811.
86E Ezhevskii, A.A.: private communication **1986**.
86H Höhne, M.: Phys. Status Solidi (b) **138** (1986) 337.
86L Lin, X.: Acta Phys. Sinica **35** (1986) 716.
86W1 Wu, E., Mao, J.C., Wu, S.X., Yan, M.X., Qin, G.G.: Phys. Lett. **118A** (1986) 347.
86W2 Wörner, R., Schirmer, O.F.: Phys. Rev. **B34** (1986) 1381.
86W3 van Wezep, D.A.: Thesis, University of Amsterdam, Netherlands **1986**.
87G1 Gregorkiewicz, T., van Wezep, D.A., Bekman, H.H.P.Th., Ammerlaan, C.A.J.: Phys. Rev. **B35** (1987) 3810.
87G2 Gorelkinskii, Yu.V., Nevinnyi, N.N., Ajazbaev, S.S.: Phys. Lett. **125A** (1987) 354.
87G3 Gorelkinskii, Yu.V., Nevinnyi, N.N.: Pis'ma Zh. Tekh. Fiz. (USSR) **13** (1987) 105.
87K van Kooten, J.J., Sieverts, E.G., Ammerlaan, C.A.J.: Solid State Commun. **64** (1987) 1489.
87S Severitt, S., Rodewald, D., Vollmer, H.: Verh. Dtsch. Phys. Ges. **22** (1987) p. HL-5.9.
87V Vlasenko, L.S., Lebedev, A.A., Taptygov, E.S., Khramtzov, V.A.: Pis'ma Zh. Tekh. Fiz. (USSR) **13** (1987) 1322.
87W Wu, E., Wu, S., Mao, J., Yan, M., Qin, G.: Solid State Commun. **61** (1987) 199.
88B von Bardeleben, H.J.: private communication **1988**.
88G Gehlhoff, W., Irmscher, K., Kreissl, J.: New Developments in Semiconductor Physics, Berlin: Springer **1988**, p. 262.
88O van Oosten, A.B., Ammerlaan, C.A.J.: Solid State Commun. **65** (1988) 1039.
88S Song, L.W., Zhan, X.D., Benson, B.W., Watkins, G.D.: Defects in Electronic Materials, Pittsburgh: Materials Research Society **1988**, p. 79.
88W1 Wu, S., Yan, M., Xu, H., Mao, J., Wu, E.: Sci. Sin. **31** (1988) 98.
88W2 Watkins, G.D.: private communication **1988**.